Diode laser induced chemical vapor deposition of WSi_x on TiN from WF_6 and SiH_4

P. Desjardins, R. Izquierdo, and M. Meunier[a)]
Groupe des Couches Minces and Département de Génie Physique, École Polytechnique de Montréal, C.P. 6079, Succ. A. Montréal, Québec H3C 3A7, Canada

(Received 17 November 1992; accepted for publication 19 January 1993)

A compact and inexpensive laser direct writing system, using a continuous wave GaAlAs diode laser array emitting 1 W at $\lambda = 796$ nm, has been developed for the deposition of WSi_x on TiN from a gas mixture of WF_6 and SiH_4. Lines 4 to 15 μm wide and 110–950 nm thick are deposited at 5 μm/s in a static reactor. The W/Si ratio in the bulk of the deposit, as measured by Auger electron spectroscopy, is between 1.1 and 1.4 for the lines deposited from a gas mixture of 1 Torr WF_6 and 3 Torr/SiH_4. In a dynamic reactor, with a flowing gas mixture of 1 sccm WF_6 and 3 sccm SiH_4 diluted in 50–150 sccm Ar, lines written at 100 μm/s are typically 4–12 μm wide and 250–800 nm thick. The W/Si ratio in the bulk of the deposit is between 1.5 and 1.8 in this case. Thickness decreases when the argon flow increases suggesting that the growth rate is limited by the transport of the reactive species, at least for a portion of the growth. A tungsten-rich top surface of the deposited layer is also observed, indicating that room temperature reactions, between the gas species and the deposited materials, continue after the deposition.

I. INTRODUCTION

Laser induced deposition of refractory metals and silicides is particularly interesting for applications in microsurgery and custom design[1–4] of microelectronic circuits. Laser chemical vapor deposition (LCVD) of tungsten from $W(CO)_6$ has been studied extensively.[5–11] In general, growth rates are small, and resistivities of the deposited films are high due to carbon and oxygen incorporation. The use of tungsten hexafluoride (WF_6) generally leads to better quality films. Tungsten has been deposited from WF_6 using ion lasers (Ar^+, Kr^+),[1–4,12–20] excimer lasers,[21–25] and CO_2 lasers.[26,27] Most of these studies relied on the reduction of WF_6 by hydrogen or by the silicon substrate. However, hydrogen reduction occurs at relatively high temperature (>400 °C),[15] and the silicon reduction is self-limited to very thin films.[14]

Silane (SiH_4) reduction of WF_6 has been recently proposed as a low temperature reaction and high deposition rate process in LCVD.[16] Black *et al.*[16] used an Ar^+ laser (488 nm) to induce the deposition of tungsten on polyimide from a gas mixture of WF_6 and SiH_4 diluted in argon. This reaction is particularly interesting because it allows one to deposit pure tungsten or tungsten silicide films, depending on the deposition conditions. However, the initiation temperature of the SiH_4 reduction reaction strongly depends on the composition of the gaseous ambient. Also, the SiH_4–WF_6 mixture is highly reactive and explosive conditions are possible.[16]

Even though many potential applications of laser processing have been demonstrated in research laboratories,[28,29] it is difficult to introduce such systems in a manufacturing environment.[30] In general, the lasers used in these processing systems are large and expensive. Also, problems related to maintenance and reliability have limited the introduction of such systems in production lines.

In contrast, semiconductor lasers are small and competitively priced. They require no maintenance and are easy to operate. The potential use of diode lasers for materials processing and device fabrication was first reported by Arjavalingam *et al.*[31] They used a 200 mW continuous wave GaAlAs diode laser array, emitting at 820 nm, to deposit gold from organometallic precursors.

The two major problems related to the use of diode lasers are the beam characteristics and the wavelength. First, the highly divergent beam is difficult to collimate and focalize. Second, high power diode lasers emit around 800 nm. As photolysis is not expected at these wavelengths, the laser beam has to induce a sufficient temperature rise to initiate a pyrolytic process. However, radiation at this wavelength is not strongly absorbed by most microelectronics materials, and such pyrolytic processes are difficult to develop.

We report here the development of a compact and inexpensive laser direct writing system for the deposition of tungsten and tungsten silicides, using a 1 W diode laser array emitting at 796 nm. Since many of the materials used in microelectronics do not strongly absorb this radiation,[32,33] the substrate has to be carefully chosen to obtain a temperature rise sufficient to induce the WF_6 reduction reaction. Because of this titanium nitride (TiN) has been selected for its optical and thermal properties. Moreover, this material is an excellent barrier layer[34] and is also used as an adhesion layer for tungsten metallization on SiO_2.[35,36] Even on such an absorbing substrate, the available diode laser power is not sufficient to induce hydrogen reduction of WF_6 since that reaction requires high temperature (>400 °C).[15] As the initiation temperature for the reduction of WF_6 by SiH_4 is about 175 °C,[16] such a process is more appropriate for diode laser induced deposition. We present here the diode laser induced CVD of WSi_x on TiN from a mixture of WF_6, SiH_4, and Ar.

[a)]Author to whom correspondence should be addressed.

 0021-8979/93/105216-06$06.00 © 1993 American Institute of Physics

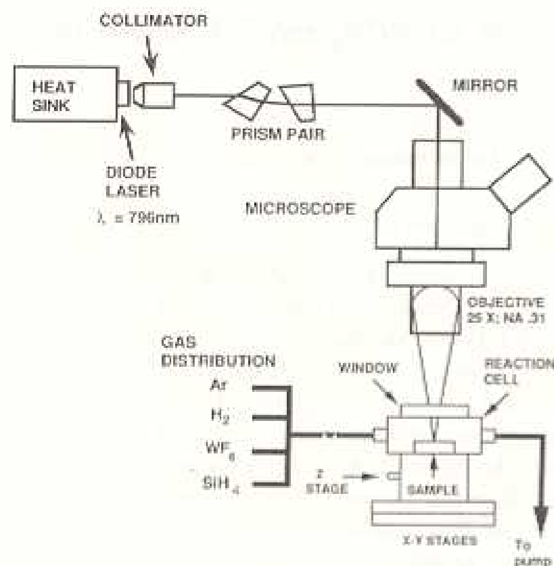

FIG. 1. Schematic diagram of the diode-laser direct writing system.

II. DIODE LASER DIRECT WRITING SYSTEM AND EXPERIMENTAL PROCEDURE

The experimental setup, schematically shown in Fig. 1, is a laser direct writing system, where the laser is used as a heat source to induce localized pyrolytic processes. The photon source is a continuous wave GaAlAs diode laser array (Spectra Diode Labs, SDL-2462-P1), emitting at $\lambda = 796$ nm, with a maximum power of 1W. The beam divergence is 10° by 40° in the two directions transverse to the propagation. The laser beam is collimated with a 0.5 numerical aperture (NA) objective and the ellipticity is reduced with a 4:1 anamorphic prism pair. The collimated beam is directed into a microscope and focused with a $25\times$ (0.31 NA), long working distance, objective. The efficiency of the optical system is 58%, yielding up to 580 mW at the substrate. The whole optical system is very compact. Indeed, the largest part is the heat sink of the diode laser.

The dimensions of the laser spot are closely related to the vertical position of the sample. Because the beam divergence is different in the two axes, an elliptic spot is obtained at the substrate. In order to maximize the laser power density, the spot area should be minimized, but, to obtain narrow lines, the length of the small axis should be decreased. Dimensions of the laser spot have been measured at various vertical positions using the scanning knife-edge technique. The smallest area is obtained when the two axis of the elliptic beam measure 12 and 93 μm, respectively, at $1/e$ of the intensity. The short axis measures 8 μm for the narrowest spot obtained, but in this case, the total area is not minimized. In most cases, deposition process was studied when the laser spot area is the smallest (12×93 μm) yielding the maximum laser power density. However, that spot area is quite large and the laser power is limited to 580 mW at the substrate. The power density is therefore relatively small and heating the substrate to the temperature necessary for the pyrolytic process may be difficult in some cases.

The substrates are 100 nm reactively sputtered TiN films deposited over a 800 nm SiO_2 film on a silicon wafer. They are degreased and dried at 120 °C for 20–30 min. They are then placed in a stainless steel reaction chamber closed by a fused silica window, and pumped to a base pressure of 10^{-2}–10^{-3} Torr. Line formation is achieved by moving the reaction chamber using computer controlled XY stages having a resolution of 0.1 μm. Lines are written at speeds ranging from 2 to 100 μm/s (the maximum velocity of the system), in the direction parallel to the long axis of the spot using different mixtures of WF_6, SiH_4, and Ar. The partial pressure of the reactive gases, WF_6 and SiH_4, is kept below 15 Torr to avoid uncontrolled reactions and explosive conditions. Argon is used as a buffer gas, and to adjust the total pressure in the reactor. The system is either operated in a static mode, where the cell is filled to the desired pressure and gas ratio before processing, or in a dynamic mode, where the gases are kept flowing at an established flow rates ratio. The substrate is at room temperature during the experiment.

In pyrolytic laser direct writing, the laser beam locally heats the surface of the substrate to induce a localized chemical vapor deposition process. The temperature rise is determined by the laser power density, and by the thermal and optical properties of the substrate and the deposited film. Since W and WSi_2 strongly absorb the diode laser radiation,[32,37] that temperature rise is critical only at the initiation of the reaction when the laser heats the bare TiN layer, and the deposition process is not self-limited by the reflectivity of the deposited layer. Because the laser power is not sufficient to induce the hydrogen reduction of WF_6, we focused on the silane reduction, which occurs at a much lower temperature.

III. RESULTS AND DISCUSSION

Characteristics of the lines obtained in both static and dynamic reactors are presented with an emphasis on the profile, structure and composition of the deposited lines.

A. Line profile: Static reactor

We have already reported some preliminary results of the diode-laser direct writing of WSi_x on TiN in a static reactor.[38,39] Figure 2 shows a scanning electron micrograph (SEM) of a typical WSi_x line deposited on TiN from a gaseous ambient, where the partial pressures of tungsten hexafluoride, $P(WF_6)$, and silane, $P(SiH_4)$, are, respectively, 1.0 and 3.0 Torr. The writing speed v is 25 μm/s and the laser power incident on the substrate P_L is 390 mW. The 4 μm width line is very uniform and the surface is smoother than that obtained with the hydrogen reduction of WF_6 using Ar^+ laser.[19]

Figure 3 shows the line thickness as a function of laser power for two different writing speeds. Lines were deposited using the same gas mixture than that used for the line pictured in Fig. 2. The width of the deposits as a function of laser power is shown in Fig. 4. Thickness is measured with a stylus profilometer (Sloan, Dektak 3030ST) and

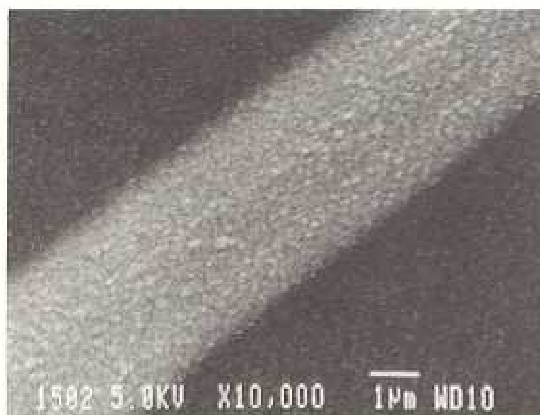

FIG. 2. Scanning electron micrograph of a WSi_x line deposited on TiN in a static reactor. $P(WF_6)=1.0$ Torr, $P(SiH_4)=3.0$ Torr, $P_L=390$ mW, and $v=25$ μm/s.

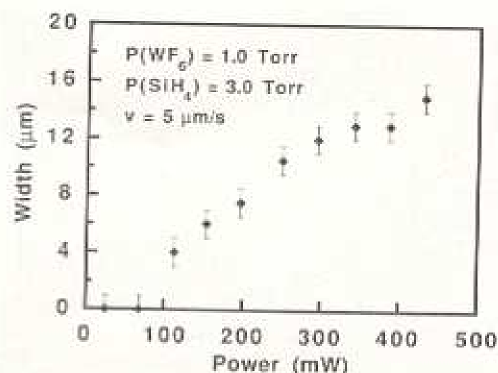

FIG. 4. Width of WSi_x lines deposited on TiN in a static reactor as a function of laser power. $P(WF_6)=1.0$ Torr, $P(SiH_4)=3.0$ Torr, and $v=5$ μm/s.

width is evaluated from micrographs. Lines written at 5 μm/s are typically 4–15 μm wide and 110–950 nm thick. Using the spot dimensions and the writing speed, average vertical growth rates of 6 to 50 nm/s are obtained. In these conditions, the threshold laser power for deposition is around 100 mW. Lines written with a laser power $P_L > 350$ mW are irregular and do not adhere well to the substrate. At these high powers, thermal stress induced by the high optical absorption of the deposit can even cause cracking of the TiN thin film.

As shown in Fig. 3, the writing speed has a strong effect on the total deposit thickness. The average vertical growth rate depends on the writing speed. The line thickness is decreased by a factor of 9 when the writing speed is increased by a factor of 5. For writing speeds larger than 25 μm/s, only nucleation traces are obtained and no continuous lines are formed. To explain that phenomena, we should recall that the instantaneous growth rate in a specific location of the sample is determined by the laser induced temperature rise which is controlled by the optical and thermal properties of the deposit–substrate system. In the present case, the reflectance of the deposit is lower than that of the substrate. We then expect a modification of the heating profile during the growth of the WSi_x film. Using the optical properties of the substrate and the deposited film, we deduce that the instantaneous growth rate is smaller at the beginning of the growth in a specified location. For different writing speeds, the final thickness of the deposit is determined not only by the total growth time but also by the heating profile which depends itself on the film thickness.

We observed, as did Black *et al.*,[16] that increasing the SiH_4 content of the gas mixture greatly increases the reactivity and the deposition rate. $P(WF_6)/P(SiH_4)$ ratio was varied from 0.2 to 10 and the reactive gases pressure from 4 to 15 Torr. In the case of silane rich mixtures, $WF_6/SiH_4 < 0.25$, deposition is difficult to control. Non-uniform lines of up to 100 μm in thickness were written at 5 μm/s. Also, deposition on the cell window readily occurs. However, for $WF_6/SiH_4 > 5$, deposition does not occur. We verified using an Ar^+ laser, that the laser power required to deposit in these gas conditions is even higher than that necessary for hydrogen reduction of WF_6. Reproducible and well controlled growth is obtained with a mixture of 1 Torr WF_6 and 3 Torr SiH_4. With an Ar buffer gas, the growth is still well controlled but the deposit thickness is reduced. When the total pressure exceeds 200 Torr, the lines are not continuous.

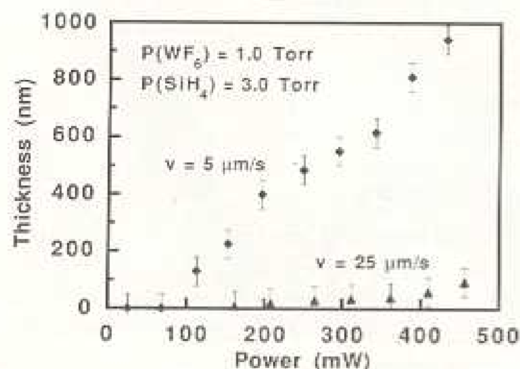

FIG. 3. Thickness of WSi_x lines deposited on TiN in a static reactor as a function of laser power for various writing speeds. $P(WF_6)=1.0$ Torr, $P(SiH_4)=3.0$ Torr, and $v=5$ and 25 μm/s.

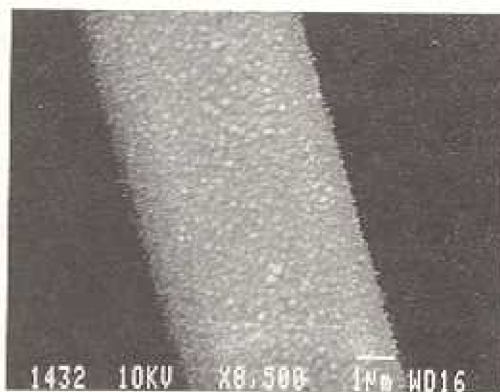

FIG. 5. Scanning electron micrograph of a WSi_x line deposited on TiN in a dynamic reactor. $f(WF_6)=1$ sccm, $f(SiH_4)=3$ sccm, $f(Ar)=50$ sccm, $P=8.9$ Torr, $P_L=360$ mW, and $v=100$ μm/s.

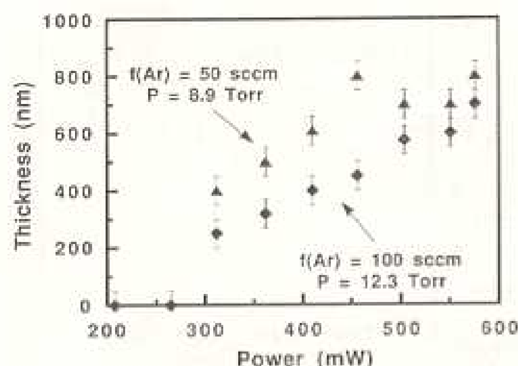

FIG. 6. Thickness of WSi_x lines deposited on TiN in a dynamic reactor as a function of laser power for various argon flows. $f(WF_6)=1$ sccm, $f(SiH_4)=3$ sccm, $f(Ar)=50$ and 100 sccm, $P=8.9$ and 12.3 Torr, and $v=100$ μm/s.

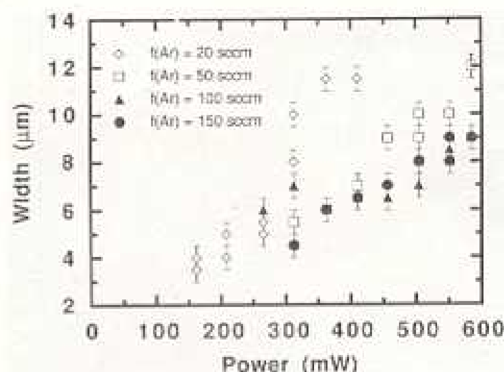

FIG. 8. Width of WSi_x lines deposited on TiN in a dynamic reactor as a function of laser power for various argon flows. $f(WF_6)=1$ sccm, $f(SiH_4)=3$ sccm, $f(Ar)=20$, 50, 100, and 150 sccm, $P=5.6$, 8.9, 12.3, and 14.3 Torr, and $v=100$ μm/s.

B. Line profile: Dynamic reactor

Lines were also deposited from a flowing gas mixture of WF_6 and SiH_4 diluted in argon. Figure 5 shows a scanning electron micrograph of a typical WSi_x line deposited at $v=100$ μm/s on TiN in a dynamic mode. This line looks very uniform. The total pressure in the reactor P is 8.9 Torr, and the flows of WF_6, SiH_4 and Ar are, respectively, $f(WF_6)=1$ sccm, $f(SiH_4)=3$ sccm, and $f(Ar)=50$ sccm. The laser power incident on the substrate P_L is 360 mW.

Line thickness as a function of laser power is shown in Fig. 6. Thickness is obtained from profilometer measurements and scanning electron micrographs of the cleaved profile of the deposits. WF_6 and SiH_4 flows are kept constant at 1 and 3 sccm, respectively, while the argon flow is 50 and 100 sccm. The total pressure in the reactor is 8.9 and 12.3 Torr in these cases. Thickness decreases when the argon flow increases. Lines of 200–800 nm in thickness are reproducibly written at 100 μm/s. This gives an average vertical growth rate of 215–860 nm/s.

Figure 7 shows the influence of the argon flow on the line thickness when the reactive gases flows and laser power are kept constant. Since we are using the same pumping speed, the total pressure in the reactor also increases with the argon flow. In the case of a small argon flow (20 sccm), the gas mixture is then highly reactive. The lines are then very thick and the process cannot be easily controlled. Reproducible and well controlled growth is obtained for a mixture of 1 sccm WF_6, 3 sccm SiH_4, and 50–150 sccm Ar. Lines written in these conditions adhere well to the TiN substrate. The effect of the argon flow on the total thickness suggests that the growth rate is limited by the transport of the reactive species, instead of the surface kinetics, for at least a portion of the growth.

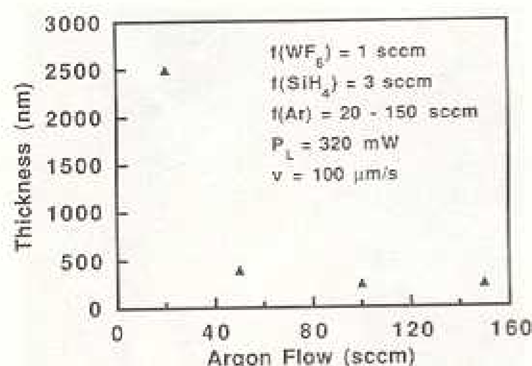

FIG. 7. Thickness of WSi_x lines deposited on TiN in a dynamic reactor as a function of argon flow. $f(WF_6)=1$ sccm, $f(SiH_4)=3$ sccm, $f(Ar)=20$, 50, 100, and 150 sccm, P=5.6, 8.9, 12.3, and 14.3 Torr, $P_L=320$ mW, and $v=100$ μm/s.

Linewidth as a function of laser power is presented in Fig. 8. Lines are written in the same conditions than those presented in Fig. 6, and are typically from 4 to 12 μm wide. For well controlled deposition conditions, where $f(Ar)\geqslant 50$ sccm, the argon content of the gas mixture has little effect on the width of the lines. In the case of small argon flows, the difficulty to control the reaction gives rise to an appreciable broadening of the deposits when $P_L>300$ mW. If there is no argon in the gas mixture, the reaction is almost impossible to control. In these conditions, large deposits on the substrate and the cell window are obtained, even at low laser power.

As mentioned previously, it is possible to focalize the laser in order to obtain a narrow, highly elliptic spot of 8 μm width. Figure 9 shows the width of the lines written in these conditions. We clearly see that the lines are narrower than those presented in Fig. 8. Deposits of 2.5 μm width were obtained. However, because the power density is reduced, higher laser powers are necessary to induce the deposition process.

C. Growth structure

Figure 10 shows a scanning electron micrograph of the cleaved profile of a typical WSi_x line. The Gaussian-like profile of the line is very uniform. We see a columnar growth structure, often observed in the chemical vapor deposition of refractory metals.[40] The top of the columns has the shape of a dome.

The surface of the deposits is smooth but we notice very often the formation of nodules as shown in Figs. 2 and

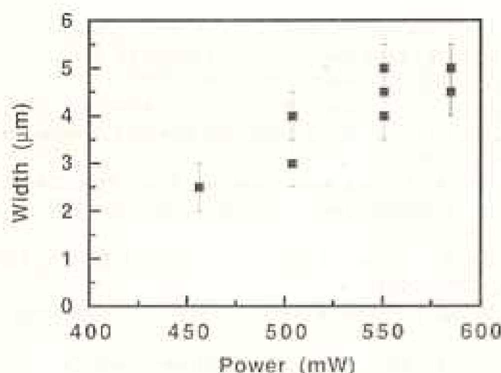

FIG. 9. Width of WSi_x lines deposited on TiN in a dynamic reactor as a function of laser power when the focalization is optimized to obtain a narrow spot. $f(WF_6)=1$ sccm, $f(SiH_4)=3$ sccm, $f(Ar)=150$ sccm, $P=14.3$ Torr, and $v=100$ μm/s.

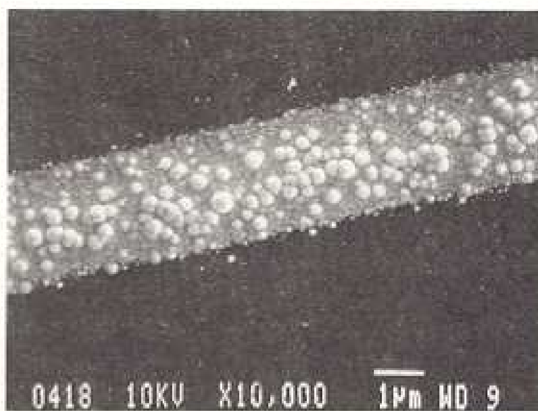

FIG. 11. Scanning electron micrograph of a WSi_x line deposited on TiN in a dynamic reactor when the focalization is optimized to obtain a narrow spot. $f(WF_6)=1$ sccm, $f(SiH_4)=3$ sccm, $f(Ar)=150$ sccm, $P=14.3$ Torr, $P_L=360$ mW, and $v=100$ μm/s.

5. These nodules are related to the columnar growth and the high deposition rate. Once the nucleus is formed, the laser light is more absorbed and the temperature rise becomes more important yielding a significant increase in the local growth rate. Because the reaction occurs at low temperature, these islands have a relatively low mobility and columnar growth is likely to occur. Note that the beam is 12 μm wide but 93 μm long. If we use an even narrower and longer beam, the formation of nodules is enhanced because the total growth time is longer. This is the case in Fig. 11 where a 2.5 μm wide line is written when the focalization is optimized to obtain a narrow, highly elliptic, spot.

D. Composition

Auger electron spectroscopy (AES) is used to determine the composition of the deposited lines. Our analysis indicates that no fluorine is incorporated in the WSi_x film within the limit of detection (1 at. %). Aside from some surface contamination attributed to atmosphere exposure between deposition and analysis, no carbon, nitrogen or oxygen are detected in the deposited film. The W/Si ratio is estimated from Si *KLL* (1620 eV) and W *MNN* (1736 eV) peak intensities. This ratio is between 1.1 and 1.4 for lines written in a static reactor and between 1.5 and 1.8 in the case of a dynamic reactor. Depth profiling measurements indicate a silicon depletion at the surface of the deposit over a few tens of nanometers. This silicon depletion has already been noticed in the preliminary results of the deposition in a static reactor.[38] This is not a measurement effect that could be attributed to the differences in sputtering efficiencies, since the sputter yield is higher for silicon than for tungsten.[41] This tungsten rich surface is directly related to the nature of the deposition process. Indeed, according to Lo,[42] many competing, temperature dependent, reactions occur between the gaseous species and the deposited materials, even at room temperature. In laser direct writing, only a fraction of the substrate is heated at a given time. A specific location of the substrate is then submitted to the temperature rise and fall. Room temperature reactions will continue at the surface of the deposit after the beam exposure. Moreover, the silicon reduction of WF_6 is thermodynamically favorable at room temperature, and it consumes silicon to produce tungsten.[42] However, this reaction is limited to a few tens of nanometers in depth by the diffusion of the silicon atoms through the tungsten layer.[14] This may explain the silicon depletion at the surface of the deposits.

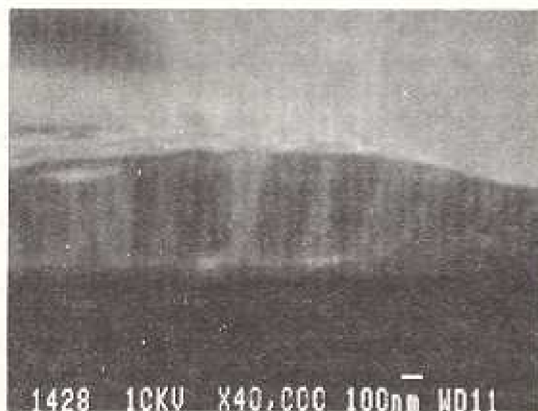

FIG. 10. Scanning electron micrograph of the cleaved profile of a WSi_x line deposited on TiN in a dynamic reactor, showing columnar grain structure. $f(WF_6)=1$ sccm, $f(SiH_4)=3$ sccm, $f(Ar)=100$ sccm, $P=12.3$ Torr, $P_L=550$ mW, and $v=100$ μm/s.

IV. CONCLUSION

We have demonstrated the possibility of using a diode laser to induce a pyrolytic deposition process in a direct writing system. Because the laser power density is limited, we concentrated on the low temperature silane reduction of tungsten hexafluoride. The low absorption by many electronic materials in the near-infrared region has limited the direct writing process to specific absorbing substrates. Lines written at 5 μm/s in a static reactor are typically 4–15 μm wide and 110–950 nm thick. In the case of a dynamic reactor, lines written at 100 μm/s are typically 4–12 μm wide and 250–800 nm thick. In addition, 2.5 μm

wide lines are written when the focalization is optimized to obtain a narrow spot. This linewidth is suitable for many microsurgery applications and for the fabrication of application-specific low density circuits such as sensors and optoelectronic devices.

The optical system is actually being improved using a higher ratio anamorphic prism pair and a higher numerical aperture microscope objective. These improvements should allow us to obtain a smaller spot and then narrower lines. Also, laser, collimator and prism pair could be integrated to the microscope. Then, instead of moving the reaction chamber, it should be possible to move the whole microscope. This is very interesting in the case of either large samples such as flat panel displays, or a sophisticated reaction chamber connected to analysis tools.

We will probably assist to the development of many diode-laser based processes in the next few years. The actual progress in the semiconductor laser technology is very encouraging. Lasers having higher power and shorter wavelength are emerging.[43–46] Furthermore, the proposed use of diode lasers in writable optical data-storage systems will stimulate the diode laser technology.[47] For all these reasons, we believe that diode lasers may play an important role in the industrial applications of laser processing.

ACKNOWLEDGMENTS

The authors thank Professor Arthur Yelon, Dr. Edward Sacher, and Maleck Tabbal of École Polytechnique de Montréal for helpful discussions, and Dr. Martine Simard-Normandin and Swandi Hambali of Northern Telecom Electronics for the TiN samples. Scanning electron micrographs and Auger analysis were done by Mr. Mario Caron from the Centre de Caractérisation Microscopique des Matériaux (CM)^2 at École Polytechnique. Technical assistance from Jean-Paul Lévesque is also acknowledged. This work was supported by the Fonds pour la Formation des Chercheurs et l'Aide à la Recherche (FCAR) du Québec and the Natural Science and Engineering Research Council (NSERC) of Canada.

[1] J. G. Black, D. J. Ehrlich, M. Rothschild, S. P. Doran, and J. H. C. Sedlacek, J. Vac. Sci. Technol. B **5**, 419 (1987).
[2] J. G. Black, S. P. Doran, M. Rothschild, and D. J. Ehrlich, Appl. Phys. Lett. **50**, 1016 (1987).
[3] C. L. Chen, J. G. Black, S. P. Doran, L. J. Mahoney, R. A. Murphy, and D. J. Ehrlich, Electron. Lett. **24**, 1396 (1988).
[4] R. F. Miracky, in *Tungsten and Other Refractory Metals for VLSI Applications IV*, edited by R. S. Blewer and C. M. McConica (Materials Research Society, Pittsburgh, PA, 1989), p. 299.
[5] D. K. Flynn, J. I. Steinfeld, and D. S. Sethi, J. Appl. Phys. **59**, 3914 (1986).
[6] N. S. Gluck, G. J. Wolga, C. E. Bartosch, W. Ho, and Z. Ying, J. Appl. Phys. **61**, 998 (1987).
[7] B. Rager and F. Bachmann, Mater. Res. Soc. Symp. Proc. **158**, 161 (1990).
[8] J. R. Swanson, F. A. Flitsch, and C. M. Friend, Surf. Sci. **226**, 147 (1990).
[9] W. Radloff, E. Below, H. Dürr, and V. Stert, Appl. Phys. A **50**, 223 (1990).
[10] F. A. Flitsch, J. R. Swanson, and C. M. Friend, Surf. Sci. **245**, 85 (1991).
[11] L. Xuebiao, Z. Jie, and Q. Mingxin, Thin Solid Films **196**, 95 (1991).
[12] Y. S. Liu, C. P. Yakymyshyn, H. R. Philipp, H. S. Cole, and L. M. Levinson, J. Vac. Sci. Technol. B **3**, 1441 (1985).
[13] Y. S. Liu, in *Tungsten and Other Refractory Metals for VLSI Applications*, edited by R. S. Blewer (Materials Research Society, Pittsburgh, PA, 1990), p. 43.
[14] J. Y. Lin and S. D. Allen, Mater. Res. Soc. Symp. Proc. **158**, 85 (1990).
[15] G. Auvert, Y. Pauleau, and D. Tonneau, Mater. Res. Soc. Symp. Proc. **158**, 155 (1990).
[16] J. G. Black, S. P. Doran, M. Rothschild, and D. J. Ehrlich, Appl. Phys. Lett. **56**, 1072 (1990).
[17] G. Q. Zhang, T. Szörényi, and D. Bäuerle, J. Appl. Phys. **62**, 673 (1987).
[18] A. Lecours, M. Meunier, and R. Izquierdo, Appl. Surf. Sci. **54**, 60 (1992).
[19] R. Izquierdo, A. Lecours, and M. Meunier, Mater. Res. Soc. Symp. Proc. **236**, 111 (1992).
[20] G. Auvert, Y. Pauleau, and D. Tonneau, J. Appl. Phys. **71**, 4533 (1992).
[21] T. F. Deutsch and D. D. Rathman, Appl. Phys. Lett. **45**, 623 (1984).
[22] A. Shintani, T. Tsuzuku, E. Nishitani, and M. Nakatani, J. Appl. Phys. **61**, 2365 (1987).
[23] A. J. P. van Maaren, R. L. Krans, E. De Haas, and W. C. Sinke, Appl. Surf. Sci. **38**, 386 (1989).
[24] R. L. Krans, C. Brands, and W. C. Sinke, Appl. Surf. Sci. **54**, 117 (1992).
[25] P. Mogyorosi, J. O. Carlsson, and M. Moradi, Appl. Surf. Sci. **54**, 46 (1992).
[26] S. D. Allen, A. B. Trigubo, and R. Y. Jan, Mater. Res. Soc. Symp. Proc. **17**, 207 (1983).
[27] S. D. Allen and A. B. Trigubo, J. Appl. Phys. **54**, 1641 (1983).
[28] *Laser Microfabrication: Thin Film Processes and Lithography*, edited by D. J. Ehrlich and J. Y. Tsao (Academic, Boston, 1989), p. 587.
[29] *Photochemical Processing of Electronic Materials*, edited by I. W. Boyd and R. B. Jackman (Academic, Londres, 1992), p. 532.
[30] F. G. Bachmann, Appl. Surf. Sci. **46**, 254 (1990).
[31] G. Arjavalingam, M. M. Oprysko, and J. E. Hurst, Jr., Mater. Res. Soc. Symp. Proc. **101**, 81 (1988).
[32] *Handbook of Optical Constants of Solids*, edited by E. D. Palik (Academic, Orlando, 1985), p. 804.
[33] *Handbook of Optical Constants of Solids II*, edited by E. D. Palik (Academic, Orlando, 1991), p. 1096.
[34] J. Hems, Semicond. Int. **13** (12), 100 (1990).
[35] Y. Nakasaki, K. Suguro, S. Shima, and M. Kashiwagi, J. Appl. Phys. **64**, 3263 (1988).
[36] M. Iwasaki, H. Itoh, T. Katayama, K. Tsukamoto, and Y. Akasaka, in *Tungsten and Other Advanced Metals for VLSI/ULSI Applications V*, edited by S. S. Wong and S. Furukawa (Materials Research Society, Pittsburgh, PA, 1990), p. 187.
[37] V. N. Antonov, Vl. N. Antonov, O. Jepsen, O. K. Andersen, A. Borghesi, C. Bosio, F. Marabelli, A. Piaggi, G. Guizetti, and F. Nava, Phys. Rev. B **44**, 8437 (1991).
[38] P. Desjardins, R. Izquierdo, and M. Meunier, Mater. Res. Soc. Symp. Proc. **236**, 127 (1992).
[39] M. Meunier, R. Izquierdo, P. Desjardins, M. Tabbal, A. Lecours, and A. Yelon, Thin Solid Films **218**, 137 (1992).
[40] S. K. Dew, T. Smy, and M. J. Brett, *Advanced Metallization for ULSI Applications*, edited by V. V. S. Rana, R. V. Joshi, and I. Ohdomari (Materials Research Society, Pittsburgh, PA, 1992), p. 85.
[41] G. E. McGuire, Surf. Sci. **76**, 130 (1978).
[42] J. S. Lo, Ph.D. thesis, University of Utah, 1973 (unpublished), p. 88.
[43] J. G. Endriz, M. Vakili, G. S. Browder, M. DeVito, J. M. Haden, G. L. Harnagel, W. E. Plano, M. Sakamoto, D. F. Welch, S. Willing, D. P. Worland, and H. C. Yao, IEEE J. Quantum Electron. **QE-28**, 952 (1992).
[44] M. Sakamoto, J. G. Endriz, and D. R. Scifres, Electron. Lett. **28**, 197 (1992).
[45] D. F. Welch and D. R. Scifres, Electron. Lett. **27**, 1915 (1991).
[46] M. A. Haase, J. Qiu, J. M. DePuydt, and H. Cheng, Appl. Phys. Lett. **59**, 1272 (1991).
[47] D. B. Carlin, Laser Focus World **28**, 77 (1992).